Photochemistry and Photobiology, 2013, 89: 1354–1361

A Versatile Near-Infrared Asymmetric Tricarbocyanine for Zinc Ion Sensing in Water†

Guillermo O. Menéndez, Cecilia Samaniego López, Elizabeth A. Jares-Erijman and Carla C. Spagnuolo*

CIHIDECAR-CONICET, Dpto. de Química Orgánica, Facultad de Ciencias Exactas y Naturales, Universidad de Buenos Aires, Ciudad Autónoma de Buenos Aires, Argentina

Received 11 March 2013, accepted 12 August 2013, DOI: 10.1111/php.12160

ABSTRACT

We have synthesized a near-infrared emissive asymmetric tricarbocyanine conveniently functionalized to improve bioconjugation. The leading structure contains a versatile derivatization point at the *meso* position for facile radical-nucleophilic aromatic substitution. We have evaluated a DPEN (*N*,*N*-di(2-picolyl)ethylendiamine) derivative of this dye as a highly selective sensor for zinc (II) in aqueous medium, which performs in an appropriate sensitivity range for biological studies. The probe was successfully conjugated to a protein-ligand model with high affinity and specificity (biotin–streptavidin technology) rendering an excellent performance of sensing. In a general strategy to obtain sensitive probes combining fluorescent nanoparticles and molecular fluorophores, a preliminary design of a supramolecular assembly derived from the conjugation of the molecular sensor to quantum dots (QDs) was also investigated. The advantages and problems of FRET-based sensors are also discussed.

INTRODUCTION

Fluorophores of the family of cyanine dyes have been widely used as fluorescent probes in the elucidation of many biological processes especially in spectroscopic techniques. One of their high-rated features is their emission in the near-infrared region (NIR) of the spectrum. This is mainly important for achieving deep penetration in tissues and to reduce to almost minimal levels the emission produced by autofluorescence, when observing cultured cells or small animals (1–4).

Among the applications of these valuable chemical tools, the monitoring and molecular imaging of biological relevant ions led to the development of multiple sensors for analytes such as Cu^{2+}, Cd^{2+}, Hg^{2+} or Zn^{2+} (5–8). A fluorescent probe capable of detecting metal ions with appropriate selectivity, sensitivity and spatial and temporal resolution can provide useful information about physiological or pathological processes related to the activity of metal ions in cells. Particularly, zinc is essential in a wide range of biological mechanisms, being the second more abundant transition metal in the human body as part of proteins (9). As a consequence, many groups directed their efforts to develop new sensors for zinc ions based on different molecular fluorophores. In recent articles, we find zinc sensors derived from a sulfamoylbenzoxadiazole fluorophore (10), coumarine (11), calixarene derivatives (12), 8-aminoquinoline (13), fluorescein (14), among other fluorescent molecules with emissive properties in the UV–Vis region. The change in the optical signal upon ion binding is mostly derived from energy or photoinduced electron transfer mechanisms.

Among those fluorescent probes for zinc capable of NIR detection, we find many examples which differ in the recognition unit: such as 6-benzoxy indol BODIPY (15), Zinhbo-5 (4), Zinhbo-1 (16), spirobenzopyran quinolone hydrazine (SPQH) (8), to mention the more recent published sensors.

Recently, we reported a detailed study on the fluorescence resonance energy transfer (FRET) process established between a fluorescent nanoparticle (Quantum dot, QD) and a tricarbocyanine dye placed on its surface through the biotin–streptavidin binding strategy (17). We proposed this supramolecular assembly as a nanosensor prototype in which we observed a remarkable quenching of QD emission by the molecules of tricarbocyanine acting as acceptor in the FRET pair. In 2008, Ruedas-Rama *et al.* reported on a zinc sensor based on semiconductor nanoparticles decorated with aza-crown ethers on their surface as recognition units, immobilized through the covalent binding of the azamacrocycle to the cysteine covering (18). The authors proposed that the observed quenching of QDs emission is due to photoinduced charge transfer. Upon addition of zinc ion, the fluorescence of the nanoparticle was recovered, turning ON the QDs. These sensors showed high sensitivity toward zinc at physiological pH with good linearity in the range 5–500 μM.

In the context of a major project involving the development of supramolecular sensing assemblies for the fluorescent detection of different analytes of biological relevance, we present the synthesis of a versatile asymmetric tricarbocyanine conveniently functionalized with a recognition site for zinc ion which also contains a biotin unit for further conjugation. The possibility of conjugation of the asymmetric tricarbocyanine to fluorescent nanoparticles to construct a supramolecular nanosensor is also discussed.

MATERIALS AND METHODS

General. All reagents were purchased from Sigma-Aldrich. NH_2–PEG–Biotin was obtained from Pierce and Qdots nanocrystals solutions from Invitrogen. NMR spectra were acquired with Bruker AC-200 or AM-500. Chemical shifts (δ) are indicated in ppm and referenced to TMS or to the corresponding deuterated solvent signal. Coupling constants are indicated in Hz. High resolution mass spectrometry (HRMS) were determined with a Bruker daltonics micrOTOF equipped with ESI ionization source and a time of flight analyzer.

*Corresponding author email: carlacs@qo.fcen.uba.ar (Carla C. Spagnuolo)
†This article is part of the Special Issue dedicated to the memory of Elsa Abuin.

Synthesis of symmetric tricarbocyanine sensor. Fifty-four milligram (68 μmol) of **1** (for synthesis see Data S1) and 33 mg (136 μmol) of DPEN were dissolved in 2 mL of anhydrous dimethylformamide (DMF) and 55 μL (395 μmol) of triethylamine were added. The solution was stirred at room temperature for 20 h protected from light. The solvent was evaporated
in vacuo leading to a deep blue residue that was purified through exclusion chromatography with Toyopearls HW40F as stationary phase and methanol as eluent. Thirty-six milligram of a deep blue solid was obtained. Yield 53%.

NMR-^{1}H (500 MHz, CD_3OD): δ 8.53 (d, J = 4.3 Hz, 2H), 8.06 (d, J = 8.5 Hz, 2H), 7.96–7.86 (m, 4H), 7.86–7.76 (m, 4H), 7.60–7.51 (m, 4H), 7.47 (d, J = 8.8 Hz, 2H), 7.43–7.29 (m, 4H), 5.95 (d, J = 12.1 Hz, 2H), 4.24 (t, J = 7.2 Hz, 4H), 4.07 (s, 4H), 3.87 (t, J = 5.5 Hz, 2H), 3.11–2.91 (m, 6H), 2.69 (t, J = 6.0 Hz, 2H), 2.33–2.22 (m, 5H), 1.90–1.83 (m, 2H), 1.82 (s, 12H), 1.49–1.24 (m, 2H).

NMR-^{13}C (125 MHz, CD_3OD) δ 168.1, 158.4, 148.8, 140.6, 137.3, 130.9, 129.8, 129.6, 128.4, 126.7, 123.8, 123.1, 122.7, 121.4, 109.9, 93.6, 67.7, 59.7, 53.8, 49.0, 38.8, 30.2, 28.7, 27.0, 25.9, 23.5, 22.3, 21.2, 13.0, 10.0.

High resolution mass spectrometry (ESI-): (M-) calc. $C_{58}H_{63}N_6O_6S_2$ 1003.4256; found 1003.4243.

Synthesis of asymmetric tricarbocyanine. A solution of *N*-(3-sulfopropyl)-1,1,2-trimethylbenzo[e]indolenine (0.145 g, 0.43 mmol), 2-chloro-1-formyl-3-(hydroxymethylen)-1-cyclohexen (0.068 g, 0.40 mmol) and 0.15 g of molecular sieves 4 Å in 15 mL of a mixture 7:3 of anhydrous *n*-butanol/benzene was refluxed under nitrogen for 2 h. When the solution turned red, a solution of *N*-(6-carboxyhexyl)-2,3,3-trimethylindolenin (0.169 g, 0.48 mmol) in 5 mL of the mixture *n*-butanol/benzene was added and refluxed for 16 h. Then, the reaction was filtered and the solvent evaporated *in vacuo*. A red–green residue was obtained which was recrystallized from ether: methanol. The mixture of tricarbocyanines obtained was purified through exclusion chromatography with Toyopearls HW40F as stationary phase and methanol as eluent. One hundred and 83 mg of a deep green solid was obtained. Yield 62%.

NMR-^{1}H (500 MHz, CD_3OD): δ 8.57 (d, J = 14.3 Hz, 1H), 8.39 (d, J = 14.0 Hz, 1H), 8.27 (d, J = 8.5 Hz, 1H), 8.03 (d, J = 8.8 Hz, 1H), 7.99 (d, J = 8.1 Hz, 1H), 7.74 (d, J = 8.9 Hz, 1H), 7.65 (ddd, J = 8.4, 6.9, 1.2 Hz, 1H), 7.50 (dt, J = 7.5, 1.3 Hz, 2H), 7.49 (dd, J = 8.0, 1.1 Hz, 1H), 7.41 (td, J = 8.0, 1.1 Hz, 1H), 7.30 (dd, J = 8.0, 0.9 Hz, 1H), 7.26 (td, J = 7.5, 0.6 Hz, 1H), 6.55 (d, J = 14.3 Hz, 1H), 6.24 (d, J = 14.0 Hz, 1H), 4.54 (t, J = 8.0 Hz, 2H), 4.15 (t, J = 7.4 Hz, 2H), 3.02 (t, J = 6.7 Hz, 2H), 2.81 (t, J = 6.0 Hz, 2H), 2.72 (t, J = 6.0 Hz, 2H), 2.33 (dt, J = 14.7, 7.0 Hz, 2H), 2.23 (t, J = 7.3 Hz, 2H), 2.02 (s, 6H), 1.96 (t, J = 5.9 Hz, 2H), 1.85 (q, J = 7.6 Hz, 2H), 1.72 (s, 6H), 1.69 (d, J = 7.6 Hz, 1H), 1.52 (dd, J = 10.1, 7.3 Hz, 3H).

NMR-^{13}C (125 MHz, CD_3OD) δ 176.2, 173.4, 150.8, 145.6, 144.7, 143.8, 142.4, 140.8,135.6, 134.0, 133.7, 132.0, 131.1, 130.6, 129.8, 129.3, 128.8, 128.7, 128.0, 126.3, 126.2, 123.4, 112.3, 112.0, 102.9, 101.7, 56.8, 55.7, 52.6, 50.4, 45.1, 44.3, 37.4, 28.4, 28.1, 27.9, 27.7, 27.5, 27.4, 26.8, 24.5, 22.2, 18.7.

High resolution mass spectrometry (ESI-): (M-) calc. $C_{43}H_{49}N_2O_5SCl$ 739.2978; found 739.2979.

Synthesis of asymmetric biotinylated tricarbocyanine sensor. Sixty milligram(81 μmol) of compound **3** and 58 mg (240 μmol) of DPEN were dissolved in anhydrous DMF. A total volume of 90 μL (640 μmol) of triethylamine was added and the reaction was kept at room temperature for 20 h protected from light. The solvent was evaporated *in vacuo* leading to a deep blue residue that was purified through exclusion chromatography with Toyopearls HW40F as stationary phase and methanol as eluent. Fifty milligram of a compound **4** as a deep blue solid was obtained. Yield 66%.

NMR-^{1}H (500 MHz, CD_3OD): δ 8.52 (d, J = 4.4 Hz, 2H), 8.06 (d, J = 8.5 Hz, 1H), 7.90 (d, J = 8.7 Hz, 2H), 7.86–7.80 (m, 2H), 7.82 (d, J = 10.6 Hz, 2H), 7.70 (d, J = 12.7 Hz, 1H), 7.55 (d, J = 7.7 Hz, 2H), 7.48 (d, J = 8.8 Hz, 1H), 7.36 (t, J = 7.5 Hz, 2H), 7.29 (dd, J = 17.8, 7.6 Hz, 2H), 7.05 (t, J = 7.5 Hz, 1H), 7.01 (d, J = 7.9 Hz, 1H), 5.98 (d, J = 11.2 Hz, 1H), 5.78 (d, J = 12.6 Hz, 1H), 4.25 (t, J = 7.3 Hz, 2H), 4.06 (s, 4H), 3.92 (t, J = 7.1 Hz, 2H), 3.84 (t, J = 5.2 Hz, 2H), 3.22 (q, J = 7.3 Hz, 2H), 3.02 (d, J = 7.4 Hz, 2H), 3.00 (t, J = 7.4 Hz, 2H), 2.70 (t, J = 5.8 Hz, 2H), 2.61 (t, J = 5.8 Hz, 2H), 2.33–2.17 (m, 4H), 1.89–1.84 (m, 2H), 1.82 (s, 6H), 1.76–1.63 (m, 2H), 1.56 (s, 6H), 1.50 (dt, J = 15.1, 7.7 Hz, 2H), 1.33 (t, J = 7.3 Hz, 2H).

NMR-^{13}C (125 MHz, CD_3OD) δ 176.9, 166.3, 158.3, 148.8, 137.3, 131.0, 129.8, 129.6, 128.4, 127.9, 126.7, 123.7, 123.1, 122.7, 122.0, 121.5, 121.4, 109.9, 108.3, 93.6, 59.6, 53.7, 46.5, 34.1, 29.3, 27.7, 27.0, 26.2, 25.9, 25.8, 24.7, 22.3, 21.1, 7.8.

High resolution mass spectrometry (ESI-): (M-) calc. $C_{57}H_{66}N_6O_5S$ 945.4743; found 945.4715.

A solution of 9 mg (9.5 μmol) of compound **4** and 6 mg (14.3 μmol) of (+)-*N*-biotinyl-3,6,9-trioxyundecanodiamine (NH_2–PEG_3–biotin, Pierce) was dissolved in 1 mL of DMF. Then, 4 μL (28.7 μmol) of triethylamine, 1.6 mg (14.25 μmol) of *N*-hydroxysuccinimide and 2.3 mg (11.4 μmol) of *N*,*N*′-dicyclohexylcarbodiimide were added. The reaction was stirred at room temperature for 10 h protected from light. The solvent was evaporated *in vacuo* leading to a residue that was purified by thin layer-preparative chromatography with RPC18 as stationary phase and methanol/water (9:1) as eluent. 3.1 mg of a compound **4** as a deep blue solid was obtained. Yield 35%.

NMR-^{1}H (500 MHz, CD_3OD): δ 8.53 (d, J = 4.4 Hz, 2H), 8.11 (d, J = 7.4 Hz, 1H), 8.06 (d, J = 8.7 Hz, 1H), 7.91 (d, J = 8.6 Hz, 2H), 7.88–7.78 (m, 2H), 7.71 (d, J = 12.5 Hz, 1H), 7.56 (d, J = 7.7 Hz, 2H), 7.49 (d, J = 8.8 Hz, 1H), 7.41–7.23 (m, 5H), 7.05 (t, J = 7.5 Hz, 1H), 7.02 (d, J = 7.9 Hz, 1H), 6.90 (d, J = 7.2 Hz, 1H), 6.00 (d, J = 13.0 Hz, 1H), 5.78 (d, J = 12.7 Hz, 1H), 4.48 (dd, J = 7.6, 4.9 Hz, 1H), 4.29 (dd, J = 7.9, 4.5 Hz, 1H), 4.26 (t, J = 7.4 Hz, 2H), 4.07 (s, 4H), 3.94 (t, J = 7.2 Hz, 2H), 3.85 (t, J = 5.5 Hz, 2H), 3.69–3.59 (m, 8H), 3.53 (t, J = 5.4 Hz, 4H), 3.20 (s, 3H), 3.01 (dd, J = 15.5, 8.6 Hz, 4H), 2.97–2.86 (m, 1H), 2.71 (t, J = 10.1 Hz, 2H), 2.62 (t, J = 6.0 Hz, 2H), 2.33–2.13 (m, 6H), 1.88–1.84 (m, 2H), 1.82 (s, 6H), 1.76–1.58 (m, 8H), 1.57 (s, 6H), 1.46 (dt, J = 22.7, 7.5 Hz, 4H), 1.37–1.18 (m, 6H), 1.04–0.88 (m, 2H).

NMR-^{13}C (125 MHz, CD_3OD) δ 174.6, 173.2, 158.3, 148.8, 141.6, 139.6, 137.3, 131.0, 129.9, 127.9, 126.7, 123.7, 123.2, 122.7, 122.0, 121.6, 121.4, 109.9, 108.3, 106.7, 70.2, 69.8, 69.2, 61.9, 60.2, 59.6, 55.6, 53.7, 48.4, 39.6, 38.9, 38.4, 35.3, 28.4, 28.1, 27.7, 27.0, 26.2, 25.9, 25.8, 25.4, 25.3, 22.3, 21.2.

High resolution mass spectrometry (ESI-): (M-) calc. $C_{75}H_{98}N_{10}O_9S_2$ 1345.6888; found 1345.6880.

Titration experiments. In this experiment, 1.96-μM solutions of sensors **2**, **4** and **5** in buffer 2-[4-(2-hydroxyethyl)piperazin-1-yl]ethanesulfonic acid (HEPES) 100 mM, 150 mM NaCl, pH 7.4 were titrated with cumulative additions of $ZnCl_2$. The absorbance changes were monitored with a UV/Vis Cary 50 spectrophotometer in 1 cm or 5 mm optical path cuvettes. The changes in the fluorescence emission were determined in a Varian Cary Eclipse.

FRET Experiments. A total volume of 300 μL of 10-nM solutions of QDs in PBS was titrated with stock solutions of **5** in PBS 1% dimethyl sulfoxide (DMSO) and the emission of QDs at 655 nm (exc. 400 nm) was monitored. The control sample consisted of a 10 nM QD solution preincubated with free biotin (150:1, biotin: QDs). For the aggregation control experiment, 300 μL of 10 nM solutions of QDs in PBS was titrated with stock solutions of different solvents (DMSO, MeCN, MeOH) 1% in PBS in the absence of the dye. Fluorescence lifetime measurements were obtained through the time correlated single photon counting method in a Horiba Jobin Yvon IBH FluoroCube-11-NLm equipped with a LED N-405L and a TBX-01-C detector. A band pass filter 655/WB20 (Omega Optical) was used in the experiments with QDs 655. The decay data were fitted to a three exponential components using the Nonlinear Model Fit routine of Mathematica (Wolfram Research) to adequately represent the time course of excited-state deactivation.

Calculation of K_d values. The values of K_d were determined with the fractional change method through Eq. (1) applied on the curves obtained from titration experiments:

$$F = \frac{X - X_0}{X_{sat} - X_0} \quad (1)$$

where X is the observed signal, X_0 is the initial signal in the absence of zinc and X_{sat} is the saturation point signal. The values are fit to Eq. (2) (see Data S1).

$$F = \frac{R_{max}[Zn^{2+}] + R_{min}K_d}{K_d + [Zn^{2+}]} \quad (2)$$

RESULTS AND DISCUSSION

Symmetric tricarbocyanine dye as sensor for zinc (II)

We synthesized a fluorescent sensor for zinc ions derived from a symmetric tricarbocyanine dye using *N*,*N*-di(2-picolyl)ethylenediamine (DPEN) as the metal chelator. This molecule has been used successfully in other molecular probes, especially for studies in live cells, due to its high selectivity for zinc among other alkaline metals that are in abundance in the cellular environment (5, 19). The complex between a fluorescent chemosensor containing DPEN and Zn(II) served as a specific probe for nucleoside polyphosphates as recently reported by Kurishita *et al.*(20).

The symmetric tricarbocyanine dye containing a chlorine atom at the *meso* position (compound **1**, Scheme 1) proved to be a versatile precursor due to the easy substitution of the halogen atom by nucleophiles such as alkoxides, amines or thiols trough radical-nucleophilic aromatic substitution reaction, S_{RN1} (see Data S1 for synthetic details). A very interesting property of this dye is that the replacement of the chlorine atom with an amine group yields aminocyanine dye with large Stokes shift (>140 nm) that makes it very suitable for fluorescent probes (21,22). Compound **2** was obtained after the reaction of **1** with DPEN (Scheme 1) as a deep blue solid with an extinction coefficient of 61000 M^{-1} cm^{-1} at 700 nm and an emission maximum at 800 nm (λ_{exc} = 700 nm).

The changes in the optical properties of probe **2** in the presence of increasing amounts of zinc (II) were studied by titration of a 1.96 μM solution of **2** in buffer HEPES, pH 7.4 using stocks solutions of $ZnCl_2$ in the same medium. Figure 1 shows the variations in the absorbance and emission spectrum: when increasing the ratio $[Zn^{2+}]/[\mathbf{2}]$ a bathochromic shift of 20 nm and an increase in 17% of the maximum absorbance peak at higher ratios is observed as well as a bathochromic shift of 20 nm of the emission maximum and a decrease in 80% of the intensity at 785 nm with subsequent additions of $ZnCl_2$.

The shift of the absorption and emission band is analyzed in detail in Fig. 2. The absorption maximum increases up to a molar ratio cation/probe of 1:1, stabilizing at 718 nm (Fig. 2a). This shift can be explained by electronic changes occurring in the unit of DPEN. In 2006, Kiyose *et al.* described the changes in the optical properties of aminotricarbocyanines as a consequence of the electron-donating ability of amine substituent in the *meso* position of the polymethine chain (5). The authors reported that the lower the electron density of the amine, the longer the wavelength of the absorption maximum, with a slight change in the emission maximum. The results provide a rational method for the molecular design of ratiometric NIR probes, based on the difference in the electron-donating ability of the amine substituent before and after binding with the analyte of interest.

Furthermore, the Fig. 2b shows the changes in the absorbance at 725 nm as a function of the molar ratio cation/probe. A gradual increasing takes place until a ratio 1:1 of $[Zn^{2+}]/\mathbf{2}$, where the signal reaches a plateau and further additions of the cation do not change the absorbance of the probe.

The bathochromic shift of the emission maximum correlates with the absorption shift upon addition of Zn^{2+} indicating the formation of a 1:1 complex. It was demonstrated by Peng *et al.* that amine-substituted tricarbocyanines undergo excited-state intramolecular charge transfer (ICT), a process that is also

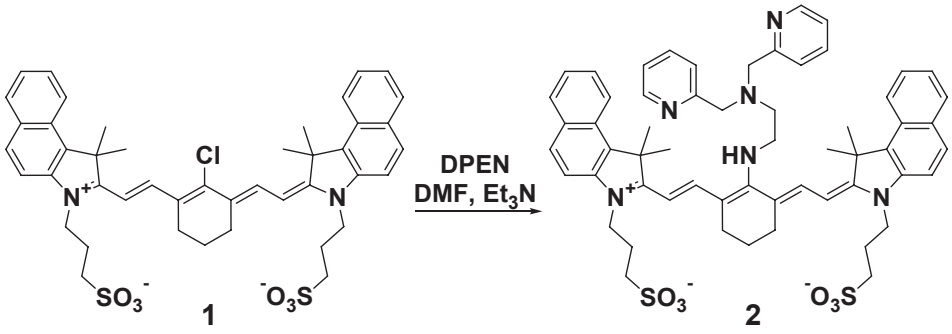

Scheme 1. Synthesis of the symmetric sensor.

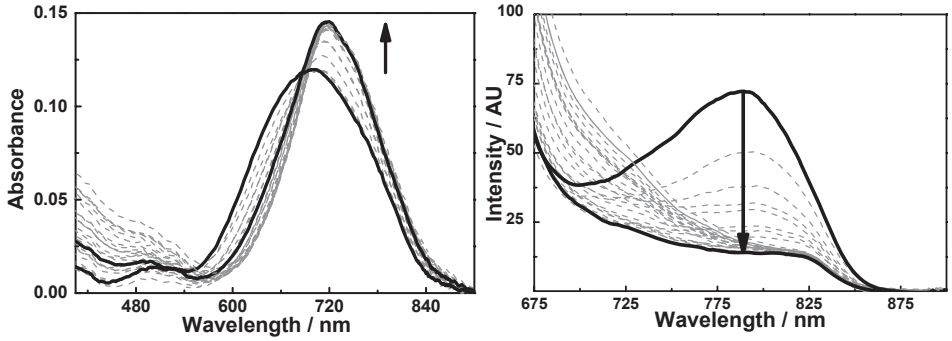

Figure 1. Change in the absorption spectra for a solution of **2** 1.96 μ in buffer HEPES 100 mM upon cumulative additions from 0 to 4 eq of Zn^{2+}.

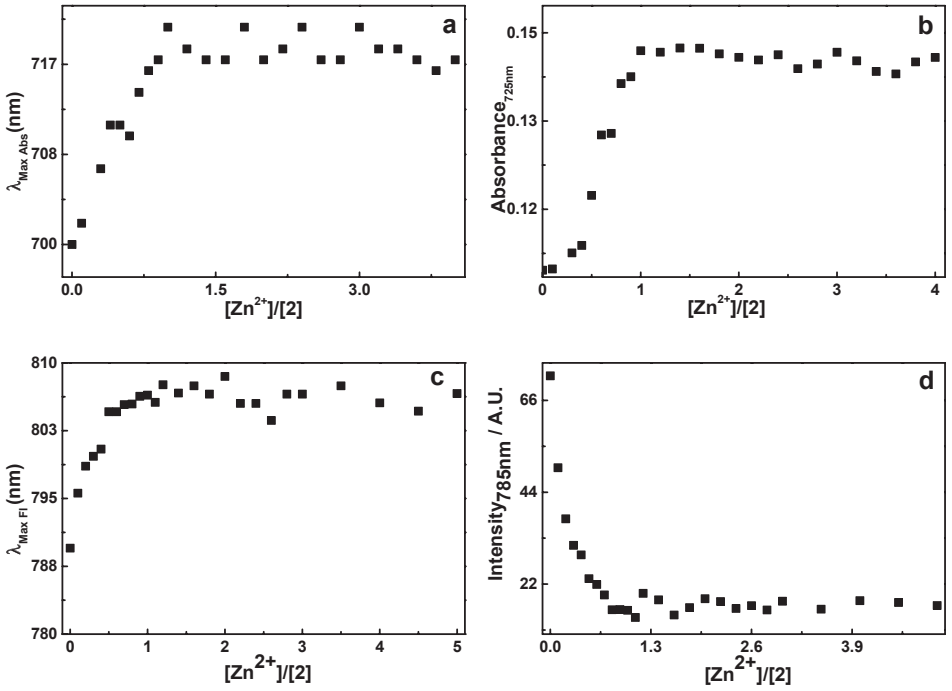

Figure 2. Titration of a solution of **2** 1.96 μM with $ZnCl_2$. Upper panel: (a) bathochromic shift of the absorbance maximum; (b) changes in the absorbance at 725 nm. Lower panel: (c) bathochromic shift of the emission maximum; (d) changes in the emission at 785 nm. λ_{exc} = 650 nm.

responsible for their large Stokes shift (23). The presence of the cation affects the ICT state, and in this case, the observed experimental behavior of the absorbance and emission maximum showing a redshift indicates a strong interaction with the acceptor group enhancing its electron-withdrawing ability. We suggest that the decrease in the emission intensity is due to the formation a nonfluorescent-twisted internal charge transfer state upon addition of the cation as a consequence of steric hindrance between the complex and benzene moieties at the ends of the tricarbocyanine skeleton.

The dissociation constants (K_d) for compound **2** were calculated with the fractional change method rendering values of 300 and 330 nM using absorbance and emission data, respectively. These values of K_d are in the nanomolar range as observed for other probes containing DPEN as the recognition unit such as ZnAF-1 (24), ZnAF-2F (25) and DIPCY (5). DIPCY is a derivative of a tricarboindolenine with a K_d value of 98 nM, lower than those obtained for **2**. The presence of naphthalene rings in **2** increases the steric hindrance accounting for the difference between the two values. Nevertheless, this is not a significant effect and the dissociation constants values calculated by emission and absorbance changes allows a dynamic range of detection between 10 nM and 1 μM for Zn^{2+}, highly convenient for its application in biological systems.

Versatile asymmetric tricarbocyanine as sensor for Zinc (II)

The synthetic strategies currently used for obtaining symmetric tricarbocyanines lead to products where only one type of functionality (such as sulfonate or carboxylic group), is included in the molecule. The presence of $-SO_3^-$ enhances water solubility of the dye, whereas the –COOH gives the possibility of further conjugation with another molecule, biomolecule or fragment of interest, expanding the performance of the sensor to more complex systems.

To have asymmetric tricarbocyanines where both functions coexist would be of great advantage where the spectral properties of the dye could be modulated by placing different heterocycles at both ends of the structure.

The general synthetic strategy is based on successive condensations of the Schiff base of the bisaldehyde of each heterocyclic precursor (26–30). The key point is to get an intermediate that could be isolated and reacted with a different heterocyclic fragment. Only two articles make use of this strategy to obtain rigid asymmetric tricarbocyanines, with different heterocyclic rings at the ends of the structure (31) or different alkyl chains (32). For example, Pham *et al.* obtained the dyes with a 10% yield, with the presence of large amounts of the symmetric product. We studied this strategy looking toward optimization.

The reaction was easily monitored by thin layer chromatography as reactants and products have different colors. From this analysis, it could be seen that the formation of the hemicyanine was never complete and the reaction favors the formation of the symmetric product. Any attempt to isolate the hemicyanine intermediate through different chromatographic techniques led to decomposition of the product. Therefore, we decided to follow the synthetic route described by Narayanan and Patonay, which follows a one pot strategy (Scheme 2) (32).

In this case, the Schiff base is replaced by 2-chloro-1-formyl-3-(hydroxymethylen) cyclohex-1-en. The reaction rate is slower allowing a two-step addition of different heterocyclic fragments. In our hands, this reaction yielded the symmetric product as a minor product, which made impossible to separate the asymmetric and symmetric dyes by recrystallization. We tried several chromatographic techniques with different stationary phases, getting excellent performance with ToyoPearls HF40W,

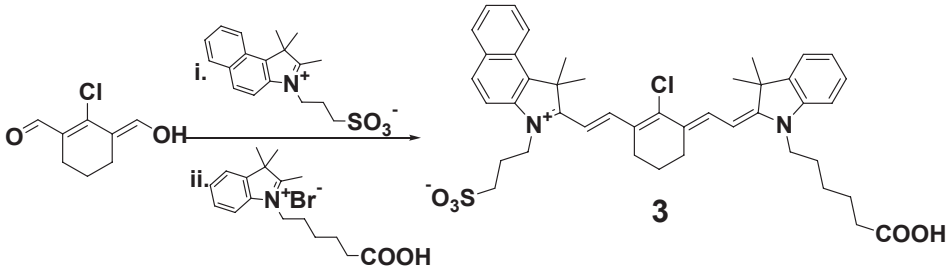

Scheme 2. Synthesis of the chlorinated asymmetric precursor.

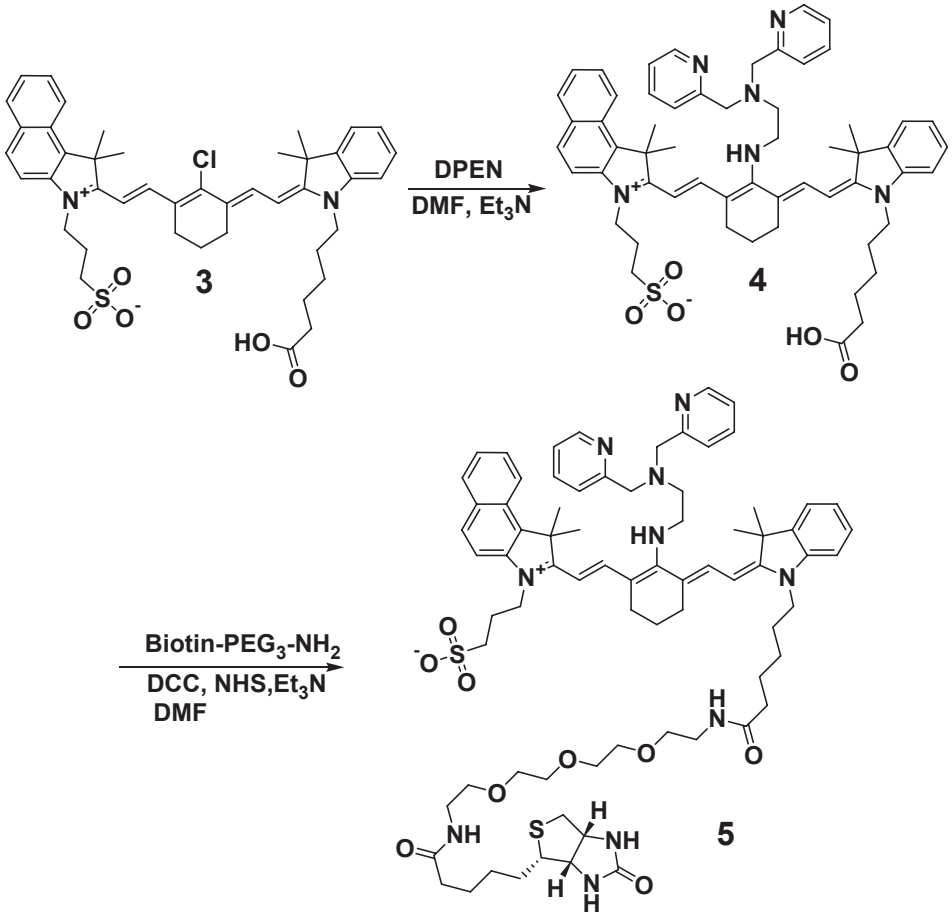

Scheme 3. Synthesis of the biotinylated asymmetric sensor.

leading to a yield of 60% on the asymmetric tricarbocyanine **3**, in a mass scale of hundreds of milligrams.

To introduce the recognition site for Zn^{2+}, the asymmetric tricarbocyanine **3** was reacted with DPEN in similar reaction conditions used for **2**, to obtain compound **4**. The presence of the carboxylate group allowed to further functionalization of the dye. We selected to conjugate a biotinylated residue in this position obtaining compound **5** (Scheme 3).

Compound **5** was spectroscopically characterized: its absorption spectrum shows a band at 780 nm (assigned to dye aggregates) besides the monomer band at 660 nm. Different solvent mixtures were tested to minimize the amount of aggregates. When the dye was complexed to streptavidin (SAv) in a 1:1 ratio in PBS 1% DMSO, the solubility of the complex fluorophore/

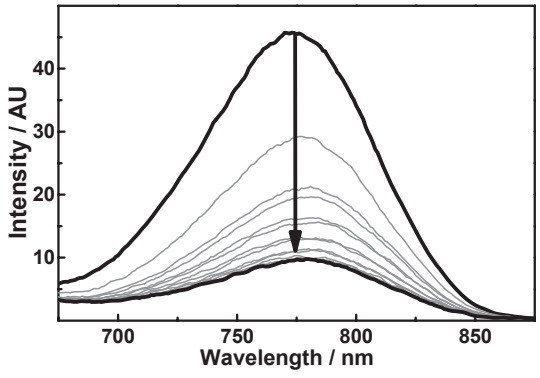

Figure 3. Changes in the emission spectra of the complex 1:1 SAv/**5** in buffer PBS 1%DMSO upon Zn^{2+} binding from 0 to 2.5eq.

protein is dictated essentially by the SAv properties. Then the complex **5**/SAv was titrated with $ZnCl_2$ and the emission spectrum after each addition of the cation was monitored (Fig. 3).

Upon each addition of zinc (II), a strong decrease in the emission intensity was observed (79%). We calculated a dissociation constant of 470 nM through the fractional change method. This value of K_d is slightly higher than the obtained for the symmetric sensor **2**, probably because of the more crowded environment around the fluorophores due to the spatial confinement on the protein surface. Nevertheless, the value is suitable for the determination of zinc ions in biological systems.

Supramolecular QD–tricarbocyanine–DPEN assembly

The unique optical properties of semiconductor nanocrystals (QDs) are well known: excellent brightness, outstanding photostability and an intrinsic insensitivity to the environmental composition. In this work, we used commercial nanoparticles composed of a semiconductor core of CdSe and a protective shell of ZnS. This core shell material is further coated with a polymer shell that allows the materials to be conjugated to biological molecules and to retain their optical properties.

A strategy for the development of fluorescent sensors with low detection limits consists of the conjugation of QDs with fluorophores capable to recognize the analyte of interest. The operation of such system is based on the modulation of the spectroscopic properties of the nanoparticles through energy transfer (FRET) or photoinduced electron transfer processes (PeT). Moreover, the affinity for the analyte is enhanced due to the multivalency effect, resulting in the multiple fluorescent molecules on the surface of the nanoparticle.

We designed a nanosensor composed of QDs with the DPEN-tricarbocyanine dye attached to their surface. We selected the emission properties of the nanoparticles to achieve a good spectral overlap with the absorption spectrum of the fluorophore. The tendency toward quenching of fluorescence upon bioconjugation of certain fluorophores is well known (33), particularly at high degrees of substitution. This is usually due to *homo*-FRET process, which is expected to be avoided with the tricarbocyanine **5**, because of its high Stokes shift (130 nm) between absorption and emission peaks.

The proof of principle of a nanosensor based on QDs and fluorophores derived from tricarbocyanines, was described in our previous work (17). We have demonstrated that upon binding to the surface of streptavidin-conjugated QDs (QD-SAv), strong quenching of the emission (90%) of the nanoparticle occurs as a consequence of a FRET process. Moreover, we showed the potential of the biotin-streptavidin technology as a strategy of conjugation, in terms of specificity, sensitivity and versatility (regarding the multiple binding sites available in the nanoparticle surface).

Previously to the conjugation onto the surface of the nanoparticles, compound **5** was conjugated to streptavidin in a ratio 1:1, and then the changes in the absorbance spectrum of the dye with the presence of zinc ion in the protein environment were studied (Fig. 4a). For each absorbance spectrum obtained, the spectral overlap (*J*) with QD655 as the FRET donor was calculated (Fig. 4). The titration with $ZnCl_2$ from 0 to 2.5 equivalents showed an important decrease in the value of *J* when increasing the ratio $[Zn^{2+}]/[\mathbf{5}]$. This result supports the viability of a fluorescent sensor based on the modulation of the efficiency of energy transfer according to the design in the protein platform.

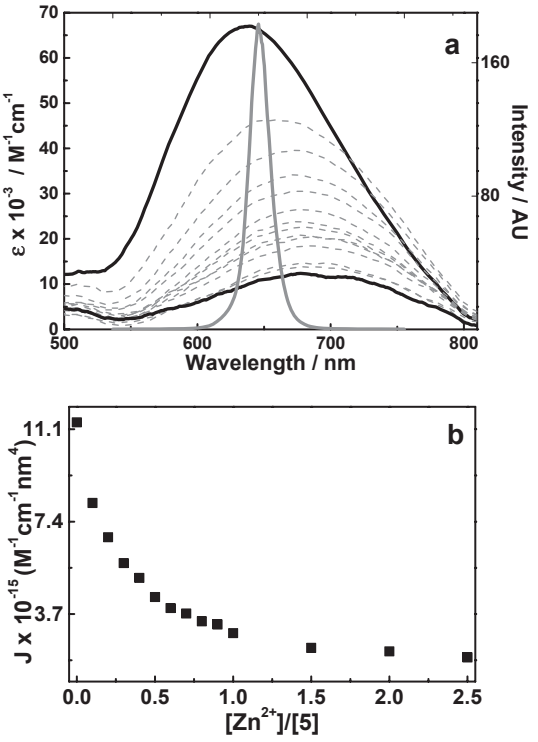

Figure 4. (a) Changes in the absorbance spectrum of the complex SAv/**5** (1:1) upon Zn^{2+} addition from 0 to 2.5 eq. In gray, the emission spectrum of QD655; (b) variation in the spectral overlap, *J*, between the nanocrystal (donor) and **5** (acceptor).

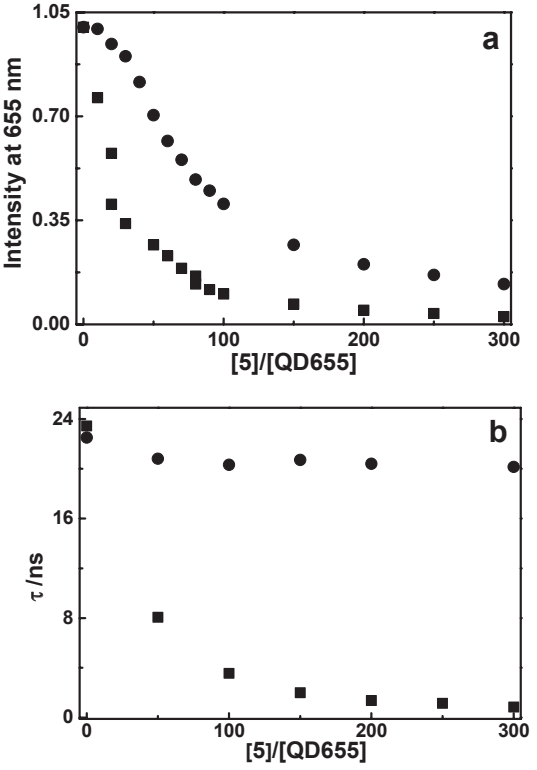

Figure 5. Titration of a solution 10 nM of QD655-SAv ITK in PBS with **5** in PBS-1%DMSO at the emission maximum (a) and mean fluorescence lifetime of the nanoparticles (b). Square points correspond to normal sample of QDs, whereas round points are control samples of QDs preincubated with biotin.

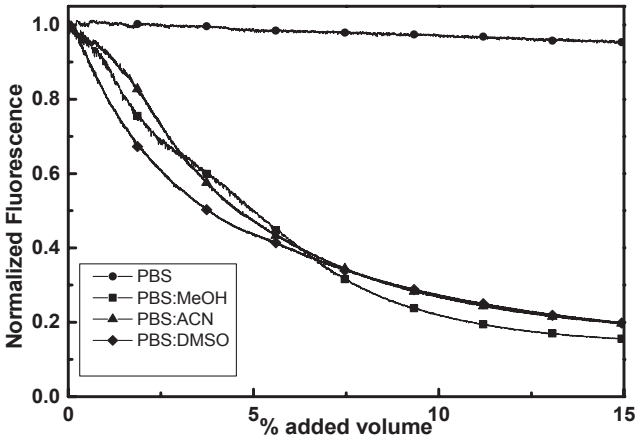

Figure 6. Titration of a 10 nM solution of QD655-SAvITK in PBS with different solvents 1% in PBS.

Afterward, a 10 nM solution of QD655-SAv ITK in PBS was titrated with **5** in PBS 1% DMSO, while the changes in the intensity of the emission of the QD at 655 nm was monitored (λ_{exc} = 400 nm). The probe **5** quenched the emission at 655 nm of the nanoparticles with high efficiency (98%) as shown in Fig. 5a (squares). This result was expected from the previous calculation of the spectral overlap and is in agreement with the quenching efficiency obtained with the *meso*-biotinylated tricarbocyanine in our previous work. A control sample consisting of QDs preincubated with biotin in a large excess (150:1) was also tested. As could be observed in Fig. 5a (circles), the control sample shows a similar response to the addition of the fluorophore, with a quenching efficiency of 87%. Therefore, it is possible to conclude that the quenching of the nanoparticles could not be attributed just to a FRET process between the QD655 and **5**. To discard the possibility of nonspecific binding of the fluorophore in the nanocrystal surface, the binding was assayed by means of time resolved fluorescence techniques (Fig. 5).

The fluorescence lifetime of QD655-SAv decreased upon addition of probe **5**, whereas in control sample (pre-saturated with biotin) stayed practically constant. The invariability in the fluorescence lifetime observed for the control sample emphasizes the specificity of the interaction between the fluorophore and the nanoparticles. Both samples undergo a loss of fluorescence emission as observed by the steady-state measurements, however, in the sensitive sample an additional process takes place which involves a depletion of the excited-state population, *e.g.* a FRET process, confirmed by time-resolved determinations. The comparison of the results obtained by the two methods leads to the conclusion that the decrease in the intensity is not only due to the conjugation of **5** on the surface of the nanoparticle but also that this difference is not a consequence of nonspecific binding. Another process is also occurring and is probably related to the presence of minimal amounts of DMSO in the stock solution of **5**. This cosolvent is necessary to solubilize **5** in aqueous solvents and to minimize the presence of dye aggregates (see Data S1), but it should be acknowledge that DMSO might also lead to nanoparticle loss by precipitation, thus affecting the intensity signal. The effect of different cosolvents (DMSO, acetonitrile, methanol) in absence of the tricarbocyanine was studied and a significative loss of the QDs'emission was also observed, which is evidence of the physical process of aggregation suffered by the nanoparticles in the presence of organic solvents (Fig. 6). This result precludes the use of cosolvent when using QDs as sensor platforms and makes the water solubility a mandatory property to consider in the molecular sensor design. The need to use DMSO to solubilize **5** could be avoided by introduction of further sulfonate groups in the heterocyclic rings, a modification which is currently under study.

CONCLUSION

We described an efficient synthesis and purification methodology of a novel asymmetric tricarbocyanine with structural versatility allowing further conjugation with interesting recognition units and different surfaces or biomolecules, at the same time. The performance of this probe as a zinc (II) sensor in water was investigated yielding suitable low dissociation constants for monitoring zinc at biological level in the NIR, a significant advantage over other sensors that work in the UV–Vis range where the background fluorescence from cellular components is not negligible.

The complexation of the biotinylated sensor to streptavidin did not significantly alter its sensing capabilities in terms of dissociation constant. The optical properties of this model assembly composed by the streptavidin and the biotinylated sensor were sensitive to the presence of zinc (II) and the fluorescence modulation of the sensor in the protein platform was achieved. The sensor was then complexed to streptavidin-conjugated QDs to investigate energy transfer properties within the conjugate as a potential nanosensor. However, studies on the emission quenching of the QD upon the sensor binding to its surface demonstrated the occurrence of secondary processes that influenced the optical signal. This preliminary results discouraged an efficient performance of the assembly as a sensor in the given conditions, *e.g.* in the presence of small amounts of DMSO. Structural modification in the tricarbocyanine molecule is in progress to avoid the use of cosolvents, thus reducing the formation of QD′s aggregates. Nevertheless, previous studies along this line of nanosensors support the general strategy described in this work.

Acknowledgements—This work is dedicated to the memory of Elizabeth Jares-Erijman and in acknowledgement of her passion for life and work, inspired leadership and unfailing support. This work has been supported in part by ANPCyT (Argentina), CONICET (Argentina), University of Buenos Aires and Max Planck Society. G.O.M. is also grateful to CONICET for a PhD fellowship.

SUPPORTING INFORMATION

Additional Supporting Information may be found in the online version of this article:

Data S1 Detailed synthesis of intermediates and NMR spectra can be found at DOI: 10.1562/2006/10.1111/php.12160.

REFERENCES

1. Akers, W. J., B. Xu, H. Lee, G. P. Sudlow, G. B. Fields, S. Achilefu and W. B. Edwards (2012) Detection of MMP-2 and MMP-9 activity *in vivo* with a triple-helical peptide optical probe. *Bioconjug. Chem.* **23**, 656–663.

2. Okuda, K., Y. Okabe, T. Kadonosono, T. Ueno, B. G. M. Youssif, S. Kizaka-Kondoh and H. Nagasawa (2012) 2-Nitroimidazole-tricarbocyanine conjugate as a near-infrared fluorescent probe for *in vivo* imaging of tumor hypoxia. *Bioconjug. Chem.* **23**, 324–329.
3. Samanta, A., M. Vendrell, S.-W. Yun, Z. Guan, Q.-H. Xu and Y.-T. Chang (2011) A photostable near-infrared protein labeling dye for *in vivo* imaging. *Chem. Asian J.* **6**, 1353–1357.
4. Xu, K., S. Sun, J. Li, L. Li, M. Qiang and B. Tang (2012) A near-infrared fluorescent probe for monitoring ozone and imaging in living cells. *Chem. Commun.* **48**, 684–686.
5. Kiyose, K., H. Kojima, Y. Urano and T. Nagano (2006) Development of a ratiometric fluorescent zinc ion probe in near-infrared region, based on tricarbocyanine chromophore. *J. Am. Chem. Soc.* **128**, 6548–6549.
6. Li, P., X. Duan, Z. Chen, Y. Liu, T. Xie, L. Fang, X. Li, M. Yin and B. Tang (2011) A near-infrared fluorescent probe for detecting copper(II) with high selectivity and sensitivity and its biological imaging applications. *Chem. Commun.* **47**, 7755–7757.
7. Yang, Y., T. Cheng, W. Zhu, Y. Xu and X. Qian (2011) Highly selective and sensitive near-infrared fluorescent sensors for cadmium in aqueous solution. *Org. Lett.* **13**, 264–267.
8. Zhu, M., M. Yuan, X. Liu, J. Xu, J. Lv, C. Huang, H. Liu, Y. Li, S. Wang and D. Zhu, (2008) Visible near-infrared chemosensor for mercury ion. *Org. Lett.* **10**, 1481–1484.
9. Vallee, B. L., K. H. And and Falchuk, (1993) The biochemical basis of zinc physiology. *Physiol. Rev.* **73**, 79–118.
10. Liu, Z., C. Zhang, Y. Chen, W. He and Z. Guo (2012) An excitation ratiometric Zn^{2+} sensor with mitochondria-targetability for monitoring of mitochondrial Zn^{2+} release upon different stimulations. *Chem. Commun.* **48**, 8365–8367.
11. Woo, H., Y. You, T. Kim, G.-J. Jhon and W. Nam (2012) Fluorescence ratiometric zinc sensors based on controlled energy transfer. *J. Mater. Chem.* **22**, 17100–17112.
12. Kumar Pathak, R., V. Kumar Hinge, A. Rai, D. Panda and C. Pulla Rao (2012) Imino–phenolic–pyridyl conjugates of calix[4]arene (L1 and L2) as primary fluorescence switch-on sensors for Zn^{2+} in solution and in HeLa cells and the recognition of pyrophosphate and ATP by [ZnL^2]. *Inorg. Chem.* **51**, 4994–5005.
13. Xie, G., P. Xi, X. Wang, X. Zhao, L. Huang, F. Chen, Y. Wu, X. Yao and Z. Zeng (2011) A highly zinc(ii)-selective fluorescent sensor based on 8-aminoquinoline and its application in biological imaging. *Eur. J. Inorg. Chem.* **2011**, 2927–2931.
14. You, Y., E. Tomat, K. Hwang, T. Atanasijevic, W. Nam, A. P. Jasanoff and S. J. Lippard (2010) Manganese displacement from Zinpyr-1 allows zinc detection by fluorescence microscopy and magnetic resonance imaging. *Chem. Commun.* **46**, 4139–4141.
15. Cao, J., C. Zhao, X. Wang, Y. Zhang and W. Zhu (2012) Target-triggered deprotonation of 6-hydroxyindole-based BODIPY: Specially switch on NIR fluorescence upon selectively binding to Zn^{2+}. *Chem. Commun.* **48**, 9897–9899.
16. Xu, Y. and Y. Pang (2011) Zn^{2+}-triggered excited-state intramolecular proton transfer: A sensitive probe with near-infrared emission from bis(benzoxazole) derivative. *Dalton Trans.* **40**, 1503–1509.
17. Menendez, G. O., M. E. Pichel, C. C. Spagnuolo and E. A. Jares-erijman (2013) NIR fluorescent biotinylated cyanine dye: Optical properties and combination with quantum dots as a potential sensing device. *Photochem. Photobiol. Sci.* **12**, 236–240.
18. Ruedas-rama, M. J. and E. A. H. Hall (2008) Azamacrozuhcycle activated quantum dot for zinc ion detection. *Anal. Chem.* **80**, 8260–8268.
19. Buccella, D., J. A. Horowitz and S. J. Lippard (2011) Understanding zinc quantification with existing and advanced ditopic fluorescent Zinpyr sensors. *J. Am. Chem. Soc.* **133**, 4101–4114.
20. Kurishita, Y., T. Kohira, A. Ojida and I. Hamachi (2012) Organelle-localizable fluorescent chemosensors for site-specific multicolor imaging of nucleoside polyphosphate dynamics in living cells. *J. Am. Chem. Soc.* **134**, 18779–18789.
21. Kiyose, K., S. Aizawa, E. Sasaki, H. Kojima, K. Hanaoka, T. Terai, Y. Urano and T. Nagano (2009) Molecular design strategies for near-infrared ratiometric fluorescent probes based on the unique spectral properties of aminocyanines. *Chem. Eur. J.* **15**, 9191–9200.
22. Peng, X., Z. Yang, J. Wang, J. Fan, Y. He, F. Song, B. Wang, S. Sun, J. Qu, J. Qi and M. Yan (2011) Fluorescence ratiometry and fluorescence lifetime imaging: Using a single molecular sensor for dual mode imaging of cellular viscosity. *J. Am. Chem. Soc.* **133**, 6626–6635.
23. Peng, X., F. Song, E. Lu, Y. Wang, W. Zhou, J. Fan and Y. Gao (2005) Heptamethine cyanine dyes with a large stokes shift and strong fluorescence: A paradigm for excited-state intramolecular charge transfer. *J. Am. Chem. Soc.* **127**, 4170–4171.
24. Hirano, T., K. Kikuchi, Y. Urano, T. Higuchi and T. Nagano (2000) Highly zinc-selective fluorescent sensor molecules suitable for biological applications. *J. Am. Chem. Soc.* **122**, 12399–12400.
25. Hirano, T., K. Kikuchi, Y. Urano and T. Nagano (2002) Improvement and biological applications of fluorescent probes for zinc, ZnAFs. *J. Am. Chem. Soc.* **124**, 6555–6562.
26. Chipon, B., G. Clavé, C. Bouteiller, M. Massonneau, P.-Y. Renard and A. Romieu (2006) Synthesis and post-synthetic derivatization of a cyanine-based amino acid. Application to the preparation of a novel water-soluble nir dye. *Tetrahedron Lett.* **47**, 8279–8284.
27. Hirata, T., H. Kogiso, K. Morimoto, S. Miyamoto, H. Taue, S. Sano, N. Muguruma, S. Ito and Y. Nagao (1998) Synthesis and reactivities of 3-indocyanine-green-acyl-1,3-thiazolidine-2-thione (icg-att) as a new near-infrared fluorescent-labeling reagent. *Bioorg. Med. Chem.* **6**, 2179–2184.
28. Lin, Y., R. Weissleder and C. H. Tung (2002) Novel near-infrared cyanine fluorochromes: Synthesis, properties, and bioconjugation. *Bioconjugate Chem.* **13**, 605–610.
29. Park, J. W., Y. Kim, K. J. Lee and D. J. Kim (2012) Novel cyanine dyes with vinylsulfone group for labeling biomolecules. *Bioconjugate Chem.* **23**, 350–362.
30. Southwick, P. L., L. A. Ernst, E. W. Tauriello, S. R. Parker, R. B. Mujumdar, S. R. Mujumdar, H. A. Clever and A. S. Waggoner (1990) Cyanine dye labeling reagents–carboxymethylindocyanine succinimidyl esters. *Cytometry* **11**, 418–430.
31. Pham, W., Z. Medarova and A. Moore (2005) Synthesis and application of a water-soluble near-infrared dye for cancer detection using optical imaging. *Bioconjugate Chem.* **16**, 735–740.
32. Narayanan, N. and G. Patonay (1995) A new method for the synthesis of heptamethine cyanine dyes – synthesis of new near-infrared fluorescent labels. *J. Org. Chem.* **60**, 2391–2395.
33. Johnson, I. D., T. Life, R. P. Haugland and M. T. Z. Spence (2010) *The Molecular Probes Handbook: A Guide to Fluorescent Probes and Labeling Technologies*, 11th edition. Life Technologies Corporation, Washington, DC.